

# Morphology, bedforms and bottom sediments of Mar do Ararapira, southern Brazil

## *Morfologia, formas de leito e sedimentos de fundo de Mar do Ararapira, sul do Brasil*

Rodolfo José Angulo<sup>ac</sup>, Maria Cristina Souza<sup>ad</sup>, Luiz Henrique Sielski<sup>be</sup>,  
Raissa Araújo Nogueira<sup>bf</sup>, Marcelo Eduardo José Müller<sup>bg</sup>

<sup>a</sup>Laboratório de Estudos Costeiros, Universidade Federal do Paraná;

<sup>b</sup>Laboratório de Estudos Costeiros, Programa de Pós-Graduação em Geologia, Universidade Federal do Paraná

<sup>c</sup>[fitoangulo@gmail.com](mailto:fitoangulo@gmail.com), <sup>d</sup>[cristinasouza2527@gmail.com](mailto:cristinasouza2527@gmail.com), <sup>e</sup>[luizion@gmail.com](mailto:luizion@gmail.com), <sup>f</sup>[raissa.nogueira@gmail.com](mailto:raissa.nogueira@gmail.com), <sup>g</sup>[medmuller@gmail.com](mailto:medmuller@gmail.com)

### Abstract

Mar do Ararapira is an unusual estuary located at the border of Paraná and São Paulo states, in a relevant area of ecological interest and where an opening of a new inlet occurred in August 2018. Differing from classical estuarine models Mar do Ararapira has three inlets, one with open sea and two with the estuarine systems of Baía de Trapandé and Baía dos Pinheiros, the latter through an artificial channel named Canal do Varadouro. Mar do Ararapira also has multiple riverine inputs and the estuary head is not well defined. This paper presents: (a) Mar do Ararapira watershed characteristics, (b) an update of coastline shift close to the inlet and (c) a characterization of the estuarine bathymetry, bottom sediments and bedforms in 2009 and 2011. Comparison of parameters before and after an opening of a new inlet will help both the management of the estuary's natural resources and the lives of the people inhabiting the surroundings. It is concluded that Mar do Ararapira corresponds to the lower part of an estuary. Its watershed extends 221.6 km<sup>2</sup> and is composed by three different morphologic sectors, which drains mountains and coastal plains. It presents a significant fresh-water input, estimated to range from 6.6 to 9.1 m<sup>3</sup>/s, and weak connectivity with its neighbor estuarine complexes. It is a shallow water body, with a mean depth of 4 m, where a deep main channel suggests intense bottom erosion by tidal currents. The ocean inlet migrates southwestward, mainly under the influence of high energy events. Prevailing bottom sediments are sand and muddy-sand. Subaqueous-sand-dunes and plane-beds are the most common bedforms at Mar do Ararapira. Three estuarine dynamically different sectors were recognized: (a) an inner sector with low tidal-current velocities and finer sediments; (b) a middle sector similar to a fluvial meander in dynamics, with higher tidal-current velocities and sandy sediments, where concave coasts are continuously eroded and convex coasts are silted; and (c) an outer sector, in which tidal-currents are segregated.

**Key-words:** bathymetry; coastline shift; inlet migration; São Paulo and Paraná coasts.

### Resumo

Mar do Ararapira é um estuário incomum localizado na fronteira do Paraná e São Paulo, em uma área relevante de interesse ecológico e onde a abertura de uma nova enseada ocorreu em agosto de 2018. Diferente dos modelos estuarinos clássicos, Mar do Ararapira possui três enseadas, um com mar aberto e dois com os sistemas estuarinos da Baía de Trapandé e Baía dos Pinheiros, este último através de um canal artificial chamado Canal do Varadouro. Mar do Ararapira também possui múltiplos insumos ribeirinhos e a cabeceira do estuário não é bem definida. Este artigo apresenta: (a) características das bacias hidrográficas de Mar do Ararapira, (b) atualização do litoral próximo à entrada e (c) caracterização da batimetria estuarina, sedimentos de fundo e formas de leito em 2009 e 2011. Comparação de parâmetros antes e depois de uma abertura de uma nova enseada ajudará tanto a gestão dos recursos naturais do estuário e as vidas das pessoas que habitam os arredores. Conclui-se que Mar do Ararapira corresponde à parte inferior de um estuário. Sua bacia hidrográfica se estende por 221,6 km<sup>2</sup> e é composta por três diferentes setores morfológicos, que drenam montanhas e planícies costeiras. Apresenta uma entrada significativa de água doce, estimada em 6,6 a 9,1 m<sup>3</sup>/s, e fraca conectividade com seus complexos estuarinos vizinhos. É um corpo de águas rasas, com uma profundidade média de 4 m, onde um canal principal profundo sugere intensa erosão do fundo por correntes de maré. A enseada do oceano migra para o sudoeste, principalmente sob a influência de eventos de alta energia. Os sedimentos de fundo predominantes são areia e areia lamacenta. Dunas e dunas de areia subaquática são as formas de leito mais comuns em Mar do Ararapira. Três setores estuarinos dinamicamente diferentes foram reconhecidos: (a) um setor interno com baixas velocidades de corrente de maré e sedimentos mais finos; (b) um setor médio semelhante a um meandro fluvial em dinâmica, com velocidades de corrente de maré mais altas e sedimentos arenosos, onde as costas côncavas são continuamente erodidas e as costas convexas são assoreadas; e (c) um setor externo, no qual as correntes de maré são segregadas.

**Palavras-chave:** batimetria; deslocamento de litoral; migração de enseadas; litoral de São Paulo e Paraná.

## 1. Introduction

Mar do Ararapira (MA) is a little known water body located at the border of Paraná and São Paulo states at the latitude of  $25^{\circ}13'18''S$  (figure 1). Five papers have been published on the inlet dynamics (Tessler & Mahiques 1993, Angulo 1993, 1999, Mihály & Angulo 2002, Angulo *et al.* 2009) and three master thesis focused on the bottom surface sediments (Kumpera 2007), on the opening of a new inlet (Müller 2010) and on its bathymetry (Nogueira 2010). Based on erosion rates of the narrow spit, which isolated MA from the open-sea, it was predicted that a new inlet would breach the spit 6 km to the north to the present mouth (Angulo *et al.* 2009, figure 2). This prediction was recently confirmed as a new inlet was opened on August 28 2018. MA is located in a relevant area of ecological interest, surrounded by protected environmental areas such as Superagüi National Park, Ilha do Cardoso State Park

and Guaraqueçaba Environmental Protection Area. On the coasts of MA, there are five small fishing villages that depend on the estuary's natural resources (Ipardes 1995). Differing from classical estuaries models Mar do Ararapira has 3 inlets connecting the estuary to the sea and to two other estuarine systems of Baía de Trapandé and Baía dos Pinheiros, the latter through an artificial channel named Canal do Varadouro. Mar do Ararapira also has multiple riverine inputs and the estuary head is not well defined.

Because the breaching of the new inlet has the potential to deeply alter the morphodynamics in the estuary, it is important to document previous morphological to be used as background information in assessing the consequences of the new hydrodynamic setting. Therefore, this paper aims to make an update of the changes of shoreline position close to the inlet, and to characterize the estuarine bathymetry, bottom sediments and bedforms.

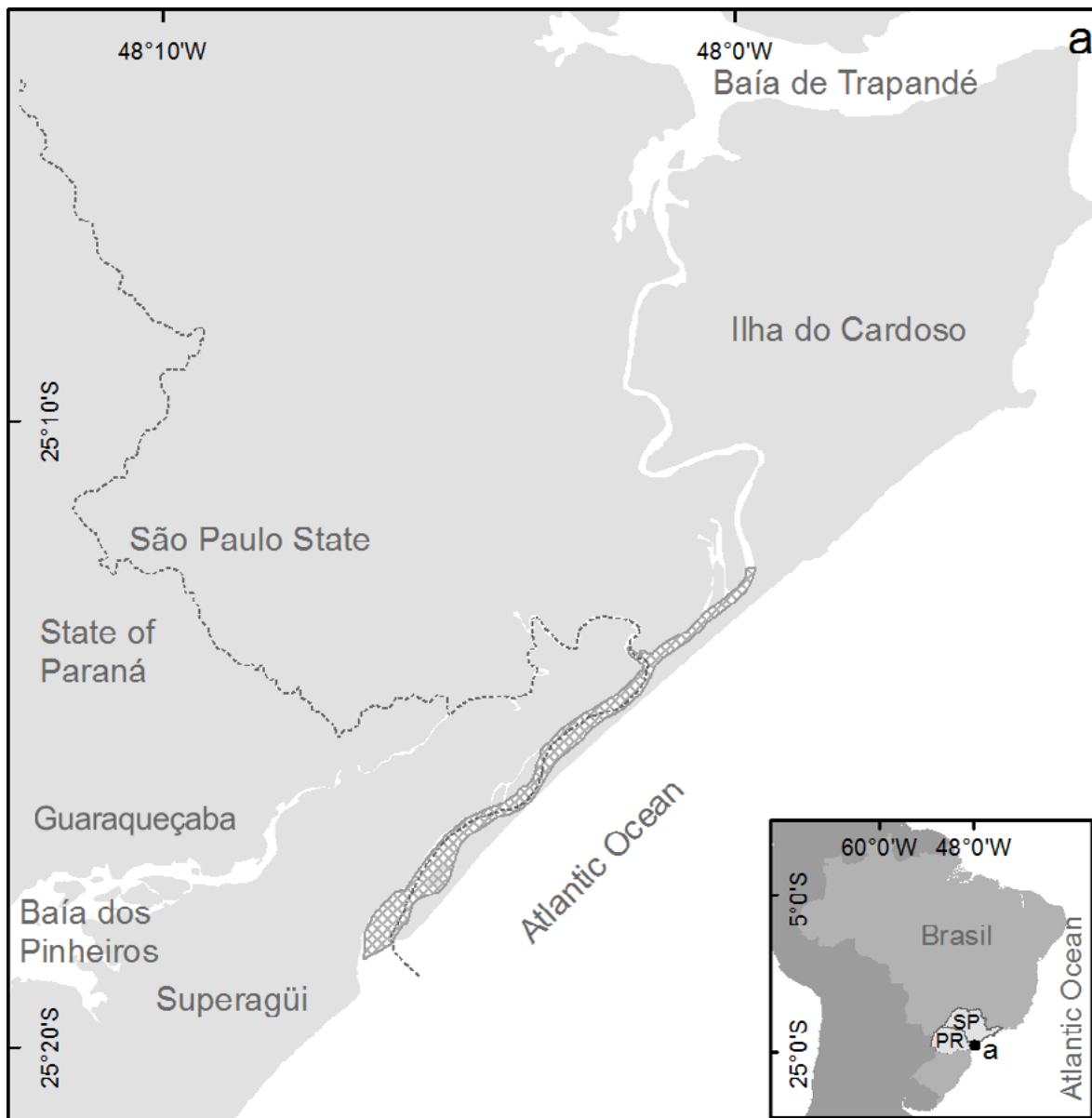


Figure 1: Study site (a), location of Mar do Ararapira (cross-hatch area), and dashed line represents interstate border between Paraná (PR) and São Paulo (SP) states.

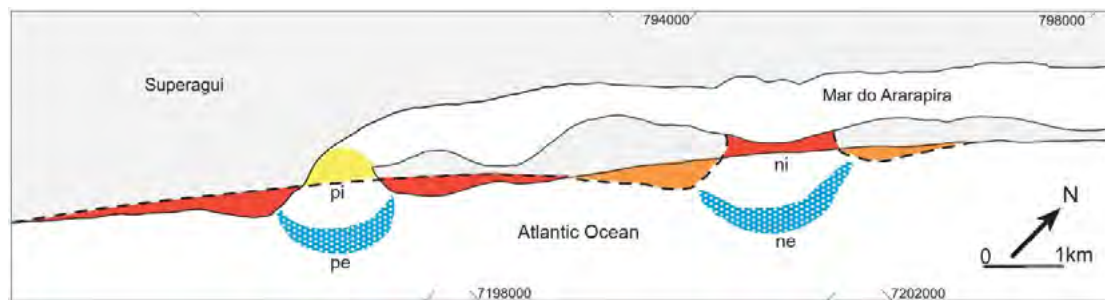


Figure 2: Predicted morphologic changes at MA after the opening of a new inlet (after Angulo *et al.* 2009). (Red) Predicted eroded areas, (orange) predicted accreted areas, (yellow) silted areas, (pi) present inlet, (ni) new inlet, (pe) present ebb-tidal delta, (ne) new ebb-tidal delta.

## 2. Regional setting

MA is a 16.5 km long, 0.5 km mean wide and 8.4 km<sup>2</sup> water body that can be defined as the lower part of an estuarine system, which includes parts of Canal do Ararapira and Varadouro River (figure 3). Its width gradually increases from 0.25 to 1.8 km in width from head to inlet (figures 3 and 4). It corresponds to the southern portion of the Cananéia-Iguape estuarine complex system (Geobrás 1966). MA estuary is connected with two other estuarine complexes: Baía de Trapandé at the north and Baía dos Pinheiros at the west. The connection is through one natural and one artificial channel (figure 3). The upper MA communicates with the Baía de Trapandé estuarine complex, through a sinuous, 22 km long, 100 to 300 m wide and mangrove-fringed tidal channel named Canal do Ararapira (figure 3). Some authors (e.g. Kumpera 2007, IBGE 1987) consider MA the southern segment of Canal do Ararapira. At the middle sector of channel, tidal-wave confluence is characterized by the presence of fine bottom sediments (Kumpera 2007, figure 3). Since the 1950s, MA communicates with the estuary of Baía dos Pinheiros through a 3.4 km long, 50 m wide artificial channel named Canal do Varadouro (figure 3). In its far northeast segment, Canal do Varadouro connects the shallow, 1 to 2 m deep tidal-channel of Baía dos Pinheiros estuarine complex to the Varadouro River, which flows to MA (figure 3).

MA is bounded by Holocene barriers (Angulo *et al.* 2009). In the northern margin lies the regressive sand barrier of the Superagui coastal plain, whereas the southern margin is delimited by the 16 km long, 20 to 700 m wide Restinga do Ararapira spit (figures 3 and 4). A new inlet is predicted to open at the narrowest part of the spit within this decade (Angulo *et al.* 2009). The present inlet, located in the southernmost part of the estuary (figure 3), has varied in width from 0.8 m to 2.0 km over the last 60 years (Tessler & Mahiques 1993, Angulo 1999, Mihály & Angulo 2002, Angulo *et al.* 2009) and has drifted southwest since spit formation started 700 to 1,100 years before present (Angulo *et al.* 2009). The inlet drifting direction has been opposite to the predominant northeast longshore drift (Tessler & Mahiques 1993, Angulo 1993, Mihály & Angulo 2002). Associated to the inlet is a wave-dominated ebb-tidal-delta (Angulo 1999).

Both coastal plain and spit include sandy beaches, foredunes ridges and tidal-flats covered with mangroves, all of them in paleo- and present forms (Angulo *et al.*

2009). Two main types of coast occur: depositional tidal-flat with mangroves related to convex estuarine margins (a), and erosional sand cliffs (b) related to concave margins.

Bottom sediments along MA and Canal do Ararapira were characterized by Kumpera (2007). According to that author, medium and fine, moderately to well sorted sand prevail in MA, being composed mainly of quartz and, subsidiarily, vegetal debris and carbonate bioclastic grains. In the outer segments of Canal do Ararapira, medium to fine sand prevail, while finer sediments with higher content of organic matter attributed to tidal-wave convergence predominate in the middle segment (Kumpera 2007). Tidal-wave convergence at Canal do Ararapira is known by the local fishermen as the *tombo das águas* (Kumpera 2007).

Local climate is controlled by the displacement of the semi-permanent South Atlantic anticyclone gyre and by polar air masses in winter (Angulo *et al.* 2016). Rainfall is seasonal, with a summer maximum and winter minimum. Mean annual rainfall on the coast of Paraná from 1997 to 2003 was of 2,363 mm (Vanhoni & Mendonça 2008). Prevailing (56 % of the time) and strongest ( $\geq 7.4$  m s<sup>-1</sup>) winds are from east, southeast and south (Dourado & Fomin 2017). Storm-surges are associated with extra-tropical cyclones over the coast (Diniz & Kousky 2004). During storm-surges, winds from southeast may reach up to 25 m s<sup>-1</sup> (Cazal *et al.* 2011).

Water temperature in MA is 20.0 to 20.5°C and salinity ranges from 27 to 34. Current velocity current ranges from 5.1 to 33.1 cm s<sup>-1</sup> on the surface, from 5.5 to 18.1 cm s<sup>-1</sup> in mid-water conditions, and 7.9 to 16.7 cm s<sup>-1</sup> at the bottom, in spring-tide conditions, in the month of July, which corresponds to winter in the southern hemisphere (Kumpera 2007).

Astronomic tides in Cananéia (25°00'S, 47°56'W) are semidiurnal, with a 1.1 m mean spring tidal range and 0.3 m mean neap tidal range (Geobrás 1966). Storm-surges are frequent (Geobrás 1966) and can reach 80 cm (Marone & Camargo 1995).

Predominant wave directions are south-southeast, southeast, south, and east-southeast (Nemes 2011). The mean significant wave height at the depth of 18 m is 1.6 m, with a maximum significant wave height of 4.8 m. The period is 8.4 s, with a maximum of 17.8 s (Nemes 2011).



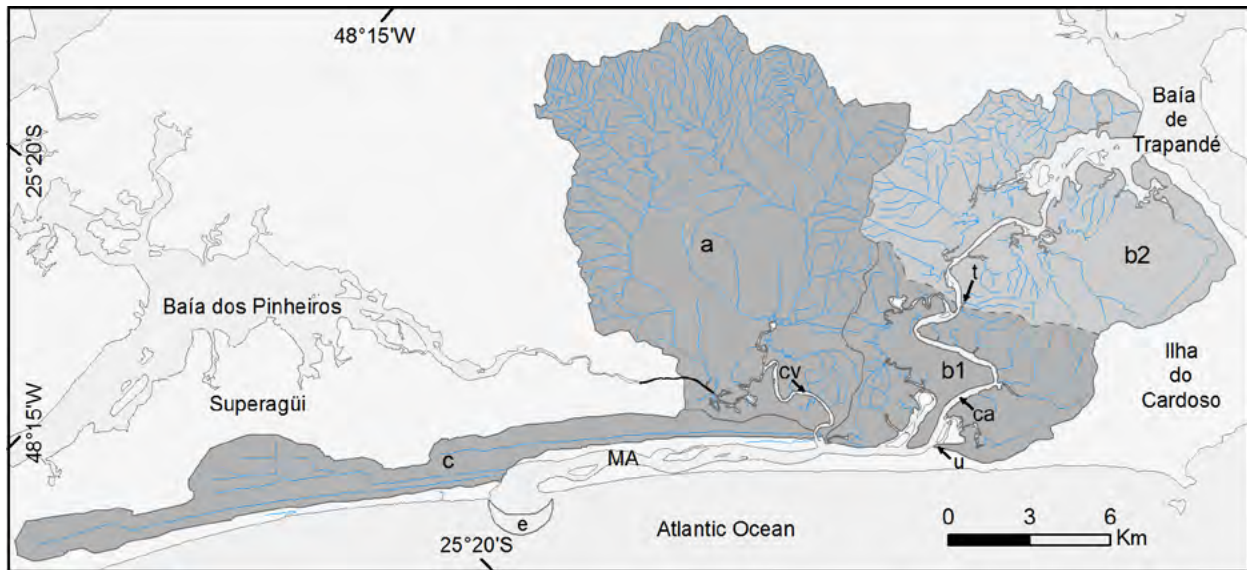


Figure 3: Watersheds of MA and Canal do Arapira, dark gray watersheds draining to MA and light gray draining to Baía de Trapandé. Watershed of (a) the Varadouro River, (b1) Canal do Arapira southern and (b2) northern sectors, and (c) Superagüi. (u) MA upper limit and (e) ebb- tidal delta; (t) approximate location of the tidal-wave confluence at Canal do Arapira; (bold line) Canal do Varadouro. Tidal channels of (vr) Varadouro River and (ca) Canal do Arapira.



Figure 4: Aerial view of MA in April 1992. (a) Superagüi coastal plain, (b) Restinga do Arapira spit, (c) Ilha do Cardoso hills, (arrow) place where the new inlet opens in 2018.

### 3. Methods

Watersheds and watershed areas were traced with geoprocessing techniques from Ariri, Cananéia and Barra do Arapira on 1:50.000 vectorial topographic charts (IBGE 1987). Watershed areas were computed by summing up all trapezoidal areas corresponding to each line segment of watershed boundary. The amount of freshwater was estimated by comparing long-term mean-specific-flow-rates (LTMSFR) of four similar neighbor watersheds where such measurements have been taken. These watersheds are similar in area, relief and precipitation rates.

Coastlines were traced by geoprocessing techniques from multiple sources. Coastlines from 1980 and 1996 were traced on georefered aerial photographs, at scales of 1:25.000 (1980) and 1:60.000 (1996). Image textural contrast between beach sand and vegetation, mainly in foredunes, was taken as boundary. The coastline from 2007 was traced with a DGPS as

one walked along the edge of foredune vegetation. Coastlines from 2013 and 2016 were traced on historical imagery from Google Earth. Coastline variation was estimated by considering the shift along an imaginary line across the inlet, from the spit end to the opposite margin, parallel to the general trend to the open-sea coastline.

Bathymetric survey was performed along the MA channel in 2009, with transects spaced at 100 m (figure 5) and a navigation speed of 3 knots, using a Garmin GPSMAP 178C echo sounder. Sampled depths were reduced to mean-sea level with the aid of a local tide gauge, with a vertical standard deviation of  $\pm 0.13$  m. The horizontal standard deviation for sampling point spacing was smaller than 1 m (Nogueira 2010). A digital bathymetric model was built as a continuous surface defined by triangulation method of triangulated irregular network (TIN). The bathymetric model was rasterized and a depth value was assigned to each raster cell.

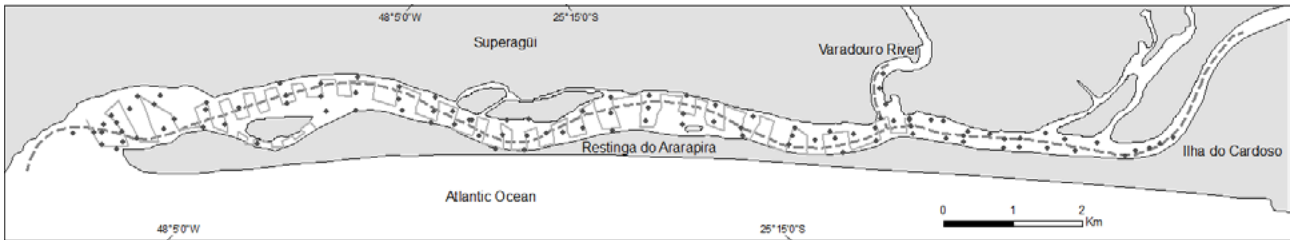


Figure 5: Location of bathymetric profiles (blue line), sampling sites (dots) and side scan lines (orange line) along MA.

One hundred and eight sediment samples were collected with a grab sampler in two campaigns in 2009 and 2011 (figure 5). The sandy fractions of the samples were dry sieved, whereas the mud fractions underwent pipetting analysis (Folk 1974, Carver 1971). Organic matter content was determined by weight loss on ignition (Wang *et al.* 2011). Calculation of textural parameters followed Pearson's technique and was performed using the Momento 4.1 software (Giannini & Nascimento Jr. 2006). An Inverse Distance Weighted (IDW) interpolation was applied, to show the variations of mean diameter and sorting degree. Sediment composition was verified on site during the sampling, and with binocular loupe on laboratory. Sediment grain morphology was determined with binocular loupe. Bottom images along the main channel were obtained with DeepVision DE340 side scan sonar, a 340 kHz transducer and 30 m lateral range, in September 2011 (figure 5). The images were post-processed with the DeepView 4.1 software. At the lower part of estuary, bedforms were also identified in Google Earth imagery. Directions of bedforms migration were inferred from asymmetric bedforms and their crest forms.

#### 4. Results and discussion

##### 4.1. Watershed area and freshwater input.

MA watershed presents contrasting relief forms, including mountain ranges and coastal plains

that can be divided in three main sectors based on physiography. One sector corresponds to the Varadouro River watershed (138.0 km<sup>2</sup>), that drains Serra Gigante and Serra do Rio Branco mountain ranges, whose altitudes reach 1,000 m (figures 3 and 6). The second sector corresponds to Canal do Ararapira watershed (118.7 km<sup>2</sup>), that drains to two different estuarine complexes, MA and Baía de Trapandé (figure 3). The limit between these two complexes is marked by a tidal-wave confluence (figure 3). Considering this limit, the watershed sector that drains to MA extends for 42.6 km<sup>2</sup>. The third watershed sector (41.0 km<sup>2</sup>) corresponds to three parallel river segments that drain the Superagüi coastal plain (figure 3 and 6): Rio da Pedra Branca and Varadouro Velho reach MA next to the inlet, while Rio da Fonte reaches Varadouro River next to the mouth (figure 3). Delimited this way, the entire MA watershed extends for 221.6 km<sup>2</sup>.

The amount of freshwater input to MA is unknown due to the lack of flow rate measurements. On the other hand, freshwater input of four neighboring watersheds similar in area, relief and precipitation rates range from 30 to 41 l/s/km<sup>2</sup> (Ipardes 1995). Therefore, in the MA watershed, flow-rate is estimated to range from 6.6 to 9.1 m<sup>3</sup>/s. Most freshwater input comes from the Varadouro River, whose watershed corresponds to 62% of the entire MA watershed (figure 3).

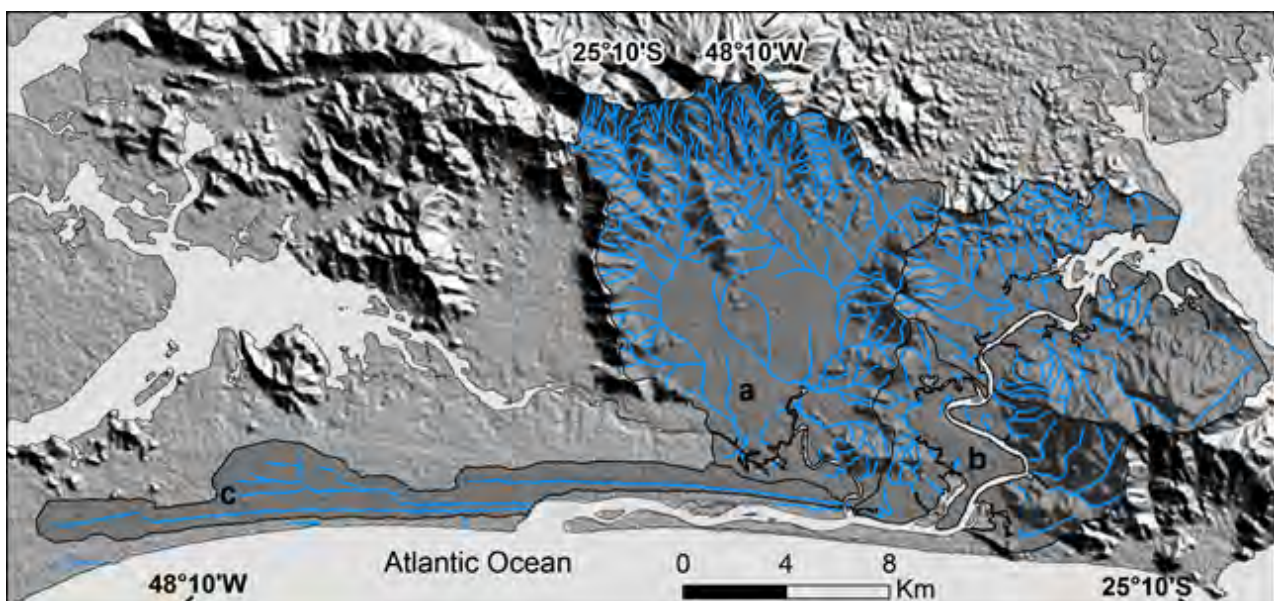


Figure 6: MA watershed relief and the main sector: (a) Varadouro River, (b) Canal do Ararapira and (c) Superagüi.



## 4.2. Inlet coastline shift

From 1980 to 2016, MA inlet shifted southwestward confirming the tendency detected in former periods (Angulo *et al.* 2009). The coastline moved 926 m southeast, and an area of 642.103 m<sup>2</sup> was accreted

in that period. At the opposite margin, the coastline shifted 395 m, and 614.103 m<sup>2</sup> of Superagüi coastal plain were eroded (figure 7). Coastline shift was episodic, with rates varying from zero up to 63.9 m.yr<sup>-1</sup> (table 1).

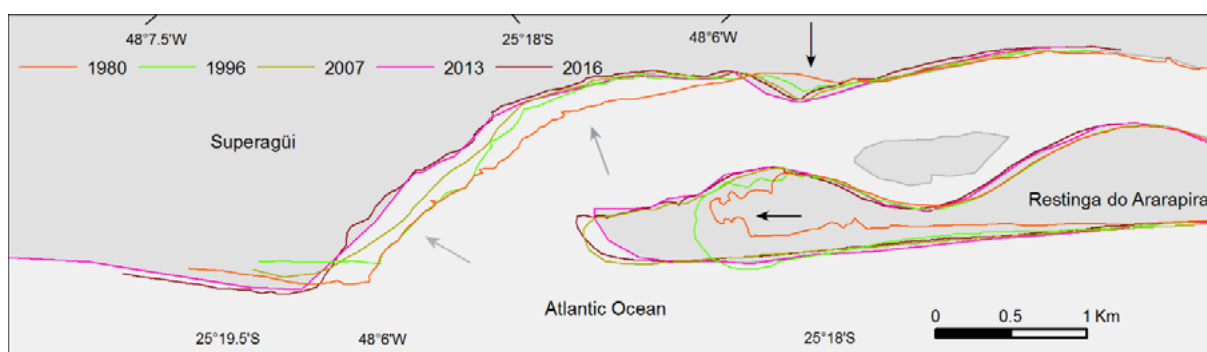


Figure 7: Coastlines next to MA inlet from 1980 to 2016; prograding (black arrows) and erosional (gray arrows) coastal sectors.

Table 1: Coastline shift rates (m.yr<sup>-1</sup>) at the MA inlet from 1980 to 2016.

Period	1980-1996	1996-2007	2007-2013	2013-2016	1980-2016
Ararapira spit	7.9	63.9	-7.0	44.7	25.7
Superagüi	0.0	-10.8	-25.2	-39.7	-11.0

## 4.3. Bathymetry, bottom sediments and bedforms

MA is a shallow lower estuary with a mean depth of 4 m. It presents a sinuous (3 to 5 km radius of curvature) main channel reaching 17 m deep (figure 8), which suggests intense bottom erosion by estuarine currents. Transversal bathymetric profiles are asymmetric, deeper near concave margins and shallower along convex margins. Maximum depths reach 7 m at outer sector of estuary (figure 8).

Bottom sediments of MA estuary are classified as sand and muddy-sand, with low content of organic matter and carbonates. Sand grains consist mainly of well-rounded to sub-angular quartz. Subsidiary constituents are heavy minerals, carbonate bioclasts (mollusk shells and shell fragments), and vegetal debris. Clay balls were observed in some samples.

Fine sand prevails along the main estuary channel (figure 9). In deeper areas near concave erosive margins, medium sand occurs. In shallow areas near convex depositional margins very fine sand and silt are present (figure 9). Very fine sand also occur upstream Varadouro River (figure 9). Sediment sorting varies from very well to very poorly sorted (figure 10). Sorting increases from inner to outer sector and from shallow to deeper areas in the estuary (figure 10).

Subaqueous sand dunes and plane beds occur in MA. Subaqueous dunes occupy mainly the outer sector of the estuary and its main channel (figure 11). Sand-dune fields consist of asymmetric, straight (2-D) and curved-crest (3-D) sand dunes with wavelengths that range from 5 to 15 m (figures 11). Sand dunes asymmetry indicates the dominance of ebb-tidal currents over bedload sediment transport. It is only along the two channels in the outer sector of MA that sand dunes migrate

landwards. Plane beds occur mainly in inner estuary, upstream the Varadouro River and in outer segments of the main channel (figure 11). A subaqueous sand cliff occurs at the erosive concave margin of estuary outer sector (figure 11).

According to bottom sediment and bedform characteristics, three main dynamic sectors can be recognized in MA estuary: (a) inner, (b) middle and (c) outer. Inner sector is located upstream the Varadouro River mouth. Middle sector lies between this river mouth and Barra do Ararapira Village. The outer sector corresponds to the area between this village and the estuary inlet (figure 11).

In inner sector of MA, plane beds and poorly sorted very-fine- and fine sand prevail, with a variable content of fine fractions and a high content of organic matter (figures 9, 10 and 11). Such characteristics indicate low tidal-current velocities.

In the middle sector, sand-dune fields prevail (figure 11). Along the main channel, very-well- to well-sorted fine to medium sand prevails (figure 9). Sediments are coarser at deeper areas next to erosive concave margins, and finer in shallower areas near depositional convex margins, where very-poorly- to poorly sorted very-fine sand and silt prevail (figures 9 and 10). This distribution of sedimentary characteristics suggests that estuarine dynamics of middle sector of MA is similar to a channelized one directional flow. Direction of sand-dune migration indicates prevalence of ebb-tidal-currents.

MA outer sector is characterized by sand-dunes fields and plane beds and by very-well- to moderately-well sorted fine sand in channels and sand bars (figures 9, 10, 11 and 12). In this sector, sand dunes migrate

in opposite directions along two channels. Bedforms are oriented upstream in the shallower sand banks by flood and oriented downstream along the main, deeper channel (figure 12).

As previously reported (e.g. Ranasinghe & Pattiaratchi 1999, Powell *et al.* 2006) estuaries morphology of the outer estuary sector changes over months, or even days, during high energy events during

which the inlet stretches and enlarges, channels shift and some areas are silted while others are eroded. Continuous southwestward inlet migration during the last millennium has caused severe erosion on the southwest coast, and deposition on the northeast coast. These sudden changes in inlet morphology are related to different wave approach-direction, the 1.1 m spring-tide range, frequent storm-surges, and to high wave-energy events.

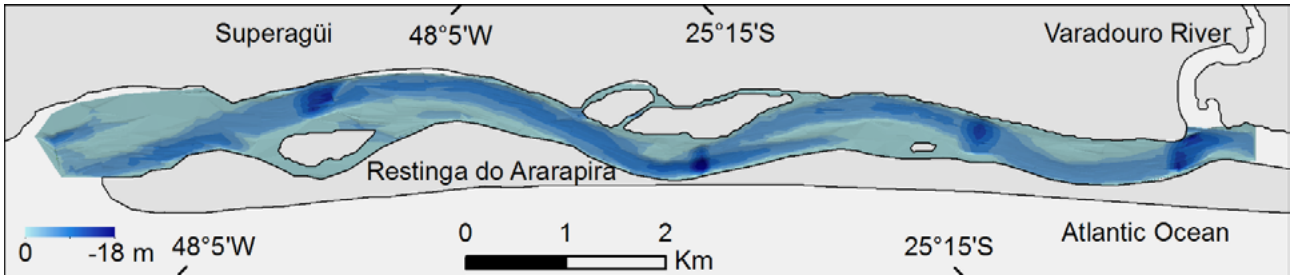


Figure 8: Bathymetry of MA.

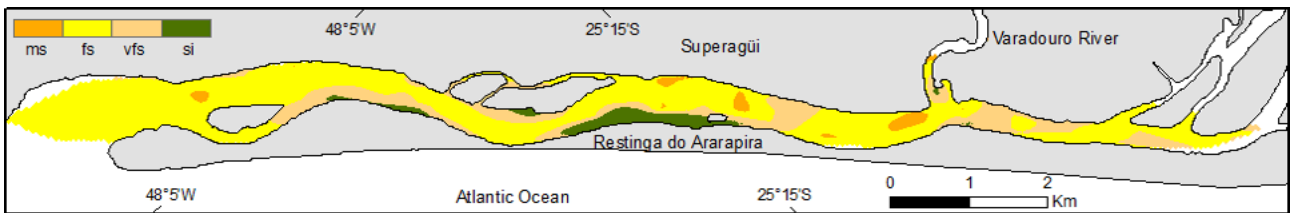


Figure 9: Mean-diameter of bottom sediments in MA: (ms) medium sand, (fs) fine sand, (vfs) very fine sand and (si) silt.

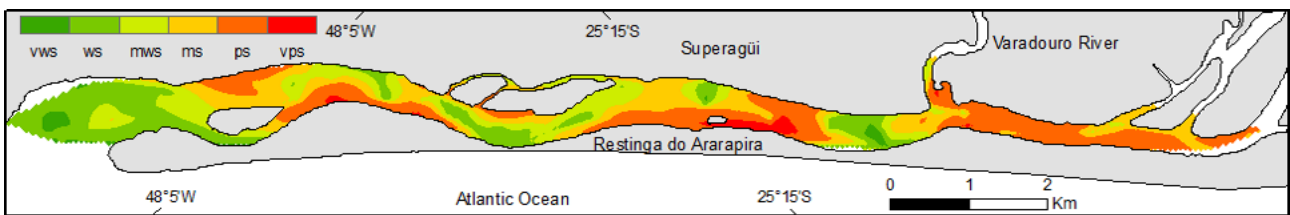


Figure 10: Sorting of bottom sediments in MA: (vws) very well sorted, (ws) well sorted, (mws) moderately well sorted, (ms) moderately sorted, (ps) poorly sorted, and (vps) very poorly sorted.

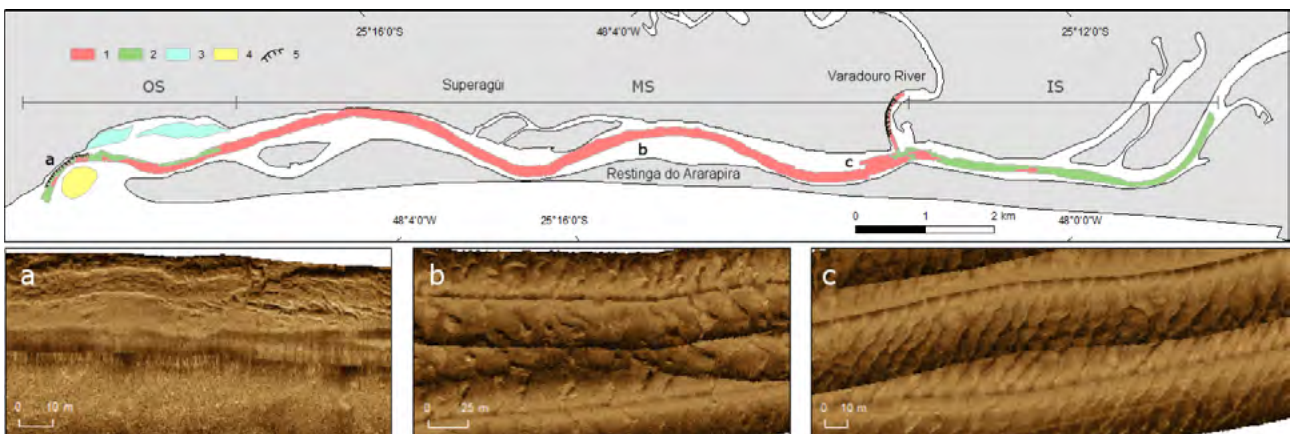


Figure 11: Sectors and bedforms in MA; (IS) inner, (MS) middle and (OS) outer sectors; (1) subaqueous-sand-dune fields and (2) plane-beds, observed at side-scan images; (3) subaqueous-sand-dune fields and (4) sand bars, observed at satellite imagery; (5) undefined bedform; (a) subaqueous sand-cliff, (b) ebb dominated curved and (c) straight-crest sand-dunes fields.



Figure 12: Outer sector of MA; (f) flood- and (e) ebb- channels, (a) sand bar and (arrows) predominant water flow direction inferred from subaqueous dune morphology (Source: Google Earth 2017).

## 5. Conclusion

Mar do Ararapira watersheds extends 221.6 km<sup>2</sup> composed by three different morphologic sectors draining mountain ranges and coastal plains. It presents significant fresh-water input, estimated to range from 6.6 to 9.1 m<sup>3</sup>/s, and low connection with its neighbor estuarine complexes. It is a shallow water body of mean depth of 4 m and a deep main channel suggesting intense bottom erosion by estuarine currents. Estuarine inlet migrates southwestward, mainly under the influence of high-energy events. Prevailing bottom sediments are sand and muddy sand. Subaqueous-sand dunes and plane beds are the main bedforms occurring at MA. Three different estuarine sectors were identified: (a) an inner sector with lower tidal-current velocities and finer sediments; (b) a middle sandy sector presenting higher tidal-current velocities, dynamically similar to a fluvial meander where concave margins are continuously eroded and convex are silted; and (c) an outer sector, in which tidal currents are segregated and the inlet migrates southwestward, mainly under influence of high energy events. MA corresponds to the lower part of an estuary; composed by the MA itself and part of Canal do Ararapira and Varadouro River, ending at tidal-convergences zones (figure 3). There are no evidences of particles and water interchange between MA and the estuaries of Baía de Trapandé and Baía dos Pinheiros. Simultaneous measurements of tides and currents at the three ends of MA should elucidate water interchange and the role of tidal convergence in the connectivity between the three estuarine systems. Likewise, observations or simulations of wind forcing estuarine circulation may reveal variations in patterns of water exchange flows.

## 6. Acknowledgments

RJA and MCS sponsored by CNPq fellowships. LHSO, RAN and MEJM sponsored by CAPES fellowships. RJA is also sponsored by Fundação Araucária senior fellowship. This study was supported by CNPq projects 558781/2008-0, 472044/2009-5, 472897/2010-1 and 477945/2012-0.

## 7. References

- Angulo R.J. 1993. Variações na configuração da linha de costa no Paraná nas últimas quatro décadas. *Boletim Paranaense de Geociências*, 41:52–72
- Angulo R.J. 1999. Morphological characterization of the tidal deltas on the coast of the State of Paraná. *Anais Academia Brasileira de Ciências*, 71(4-II):935-959.
- Angulo R.J., Souza M.C., Müller M.E. 2009. Previsão e consequências da abertura de uma nova barra no Mar do Ararapira, Paraná-São Paulo, Brasil. *Quaternary and Environmental Geosciences*, 1(2):67-75.
- Angulo R.J., Borzone C.A., Noernberg M.A., Quadros C.J.L., Souza M.C., Rosa L.C. 2016. The State of Paraná beaches. In: Short A.D & Klein A.H.F. (eds.), *Brazilian Beach Systems*, Coastal Research Library 17, Springer, Switzerland, Dordrecht, 419-464., ISBN: 978-3-319-30392-5. [https://doi.org/10.1007/978-3-319-30394-9\\_16](https://doi.org/10.1007/978-3-319-30394-9_16)
- Carver R.E. 1971. *Procedures in sedimentary petrology*. Wiley-Interscience, New York, 653p.
- Cazal H.G.S.V, Fomin I.M., Oliveira B.A., Sutil U.A., Oliveira E., Dourado M.S. 2011. Caracterização Sazonal da Precipitação e do Vento no Litoral Paranaense. In: 14th Congresso Latino-Americano de Ciências do Mar, Balneário Camboriú, Brazil, CD-ROM.
- Diniz F.A., Kousky E.V. 2004. Ciclone no Atlântico Sul – análise sinóptica e observação. In: 13th Anais Congresso Brasileiro de Meteorologia, Fortaleza, Brazil CD-ROM



- Dourado M.S., Fomin I.M. 2018. Estado médio e variabilidade da atmosfera do litoral paranaense. *Revista Brasileira de Meteorologia*, accepted.
- Folk R.L. 1974. *Petrology of sedimentary rocks*. Austin. Hemphill Publ. 184p.
- Geobrás S/A. 1966. Complexo Valo Grande, Mar Pequeno e Rio Ribeira de Iguape. Technical report, Engenharia e Fundações para o serviço do valo do Ribeira do Departamento de Águas e Energia Elétrica/SP, São Paulo, 222p.
- Giannini P.C.F., Nascimento Jr. D.R. 2006. Momento 4.1.xls. Programa de computador. Laboratório de Petrografia Sedimentar. Instituto de Geociências, Universidade de São Paulo, São Paulo.
- Hellweger F.L., Blumberg A.F., Schlosser P., Ho D.T., Caplow T., Lall U., Li H., 2004. Transport in the Hudson estuary: A modeling study of estuarine circulation and tidal trapping. *Estuaries* 27:527–538. <https://doi.org/10.1007/BF02803544>
- IBGE – Instituto Brasileiro de Geografia e estatística. 1987. Ariri. Regiões Sudeste e Sul do Brasil, escala 1:50.000, folha SG.22-X-D-III-2, Secretaria de Planejamento da Presidência da República, Rio de Janeiro-RJ.
- Ipardes - Instituto Paranaense de Desenvolvimento Econômico e Social. 1995. Diagnóstico ambiental da APA de Guaracema. Curitiba, 166 p, 11 mapas.
- Kumpers B.S. 2007. Contribuição ao processo sedimentar atual no Canal do Arapira, sistema estuarino-lagunar de Cananéia-Iguapé (SP). Dissertação de mestrado, Pró-Graduação em Oceanografia Química e Geológica, Instituto Oceanográfico, Universidade de São Paulo, 118p., available at <http://www.teses.usp.br/teses/disponiveis/21/21133/tde-01072008-102612/pt-br.php>
- Marone E., Camargo R. 1995. Efeitos da maré meteorológica na baía de Paranaguá, PR. *Nerítica*, Curitiba, 8:71-81.
- Mihály P., Angulo R.J. 2002. Dinâmica da desembocadura do Mar do Arapira. *Revista Brasileira de Geociências*, 32:(2):217-222.
- Müller M.E.J. 2010. Estabilidade morfo-sedimentar do Mar do Arapira e consequências da abertura de uma nova barra. Pós-Graduação em Geologia, Universidade Federal do Paraná, Curitiba, Dissertação de Mestrado, 75p., available at <http://acervodigital.ufpr.br/handle/1884/39718/browse?value=M%C3%BCller%2C+Marcelo+Eduardo+Jos%C3%A9&type=author>
- Nemes D.D. 2011. Caracterização das ondas de superfície na plataforma interna do estado do Paraná. Dissertação de Mestrado, Centro de Estudos do Mar, Universidade Federal do Paraná, Curitiba, 134 p., available at <http://acervodigital.ufpr.br/handle/1884/284/browse?value=Nemes%2C+Douglas+Duarte&type=author>
- Nogueira R.A. 2010. Caracterização batimétrica do mar do Arapira, litoral sul de São Paulo e litoral norte do Paraná. Monografia, Centro de Estudos do Mar, Universidade Federal do Paraná, 74p.
- Nogueira R.A. 2013. Caracterização dos sedimentos e das feições de fundo do Mar do Arapira, litoral sul do Brasil, Pós-Graduação em Geologia, Universidade Federal do Paraná, Curitiba, Dissertação de Mestrado, 71p., available at <http://acervodigital.ufpr.br/handle/1884/284/browse?value=Nogueira%2C+Raissa+de+Ara%C3%BAjo&type=author>
- Powell M.A., Thieke R.J., Mehta A.J. 2006. Morphodynamic relationships for ebb and flood delta volumes at Florida's tidal entrances. *Ocean Dynamics*, 56:295-307. doi 10.1007/s10236-006-0064-3
- Ranasinghe R., Pattiaratchi C. The seasonal closure of tidal inlets: Wilson Inlet – a case study. *Coastal Engineering*. 37:37-56
- Tessler M.G., Mahiques M.M. 1993. Utilization of coastal geomorphic features as indicators of longshore transport: Examples of the southern coastal region of the State of São Paulo, Brazil. *Journal of Coastal Research*, 9:823-830.
- Traynum S., Styles R. 2008. Exchange Flow between Two Estuaries Connected by a Shallow Tidal Channel. *J. Coast. Res.* 245:1260–1268. <https://doi.org/10.2112/07-0840R.1>
- Vanhoni F., Mendonça F. 2008. O clima do litoral do estado do Paraná. *Revista Brasileira de Climatologia*, 3-4: 49-63.
- Wang Q., Li Y., Wang Y. 2011. Optimizing the weight loss-ignition methodology to quantify organic and carbonate carbon of sediments from diverse sources. *Environ. Monit. Assess.* 174:241–257. <https://doi.org/10.1007/s10661-010-1454-z>
- Wang Y., Castelao R.M., Di Iorio D. 2017. Salinity Variability and Water Exchange in Interconnected Estuaries. *Estuaries and Coasts* 40:917–929. <https://doi.org/10.1007/s12237-016-0195-9>
- Warner J.C., Schoellhamer D., Schladow G., 2003. Tidal truncation and barotropic convergence in a channel network tidally driven from opposing entrances. *Estuar. Coast. Shelf Sci.* 56:629–639. [https://doi.org/10.1016/S0272-7714\(02\)00213-5](https://doi.org/10.1016/S0272-7714(02)00213-5)
- Wong K.-C. 2002. On the spatial structure of currents across the Chesapeake and Delaware Canal. *Estuaries and Coasts* 25:519–527. <https://doi.org/10.1016/j.dsr.2004.07.022>

---

Recebido em 17 de maio de 2018

Aceito em 15 de março de 2019